Version of Record: https://www.sciencedirect.com/science/article/pii/S0141813019332350
Manuscript_f63dd8bfbdbec3aaede75408728ff541

In silico design and *in vitro* analysis of a recombinant trivalent fusion protein candidate vaccine targeting virulence factor of *Clostridium perfringens*

Camellia katalani[1] Ghorbanali Nematzadeh[1*], Gholamreza Ahmadian[3*], Jafar Amani[4], Ghafar Kiani[2] and Parastoo Ehsani[5]

[1]Sari Agriculture Science and Natural Resource University (SANRU), Genetics and Agricultural Biotechnology Institute of Tabarestan (GABIT),

[2]Sari Agriculture Science and Natural Resource University (SANRU),

[3]Department of Industrial and Environmental Biotechnology, National Institute of Genetic Engineering and Biotechnology (NIGEB)

[4]Applied Microbiology Research Center, Baqiyatallah University of Medical Sciences

[5] Department of Molecular Biology, Pasteur Institute of Iran

[*] Corresponding Author: Gholamreza Ahmadian.

Department of Industrial and Environmental Biotechnology, National Institute of Genetic Engineering and Biotechnology, Pajoohesh BLVD, Tehran-Karaj HWY, km 15, Tehran, Iran. Postal code: 1497716316, ahmadian@nigeb.ac.ir
Tel: (+9821) 44580-351 and (+9821) 912-4187608
Fax: (+) 44580-366

[*]Co-corresponding Author: Ghorbanali Nematzadeh, [1]Sari Agriculture Science and Natural Resource University (SANRU), Genetics and Agricultural Biotechnology Institute of Tabarestan (GABIT), Sari, Iran, gh.nematzadeh@sanru.ac.ir
P.O.BOX: 578
Tel: (+9811)33687744
Fax: (+9811)33687747

In silico design and *in vitro* analysis of a recombinant trivalent fusion protein candidate vaccine targeting virulence factor of *Clostridium perfringens*

Abstract

Necrotic enteritis (NE) is a multifactorial disease in broiler that is caused by colonization of *Clostridium perfringens* in their gastrointestinal tract. Recently several immunogenic proteins from virulent *C. perfringens* have been considered as vaccines to provide protection against NE. In this study, a novel trivalent fusion protein including immunogenic epitopes of three virulence factors of, NetB, alpha toxin and a metallopeptidase protein (NAM) was designed using *in silico* studies. Circular dichroism spectra was applied for determination of secondary structure and folding properties of the purified recombinant NAM (rNAM) expressed in *E. coli*. The antigenicity of rNAM was confirmed by induction of immune response in rabbit and neutralization experiments of the toxins in cell culture studies. To this end, anti-rNAM antisera neutralized the crude toxins produced by a wild type virulent *C. perfringens* strain using chicken hepatocellular carcinoma (LMH) cell lines. The cells were exposed to a mixture of anti-rNAM antisera and 2×LD50 doses of the toxins. The result showed 94% viability of the cells against the crude toxins, in the presence of anti-rNAM antisera. Our study suggests that combination of metallopeptidase protein along with alpha toxin and NetB toxins is a potent immunogen which is able to neutralize the toxicity of crude extracellular toxins. The recombinant chimeric NAM could be a suitable and effective subunit vaccine candidate to prevent NE disease caused by *C. perfringens*.

Key words: immunogenic protein, Necrotic enteritis, fusion protein

1. Introduction

Necrotic enteritis, a gastrointestinal disease of chickens, is one of the economically devastating disease caused by *Clostridium perfringens* that considered as important threat in poultry industry worldwide [49, 50]. *C. perfringens*, at low levels, exists in the bird's intestine as bacterial flora. However, imbalance in the bacterial composition of the intestine following damage caused by *Coccidia*, or change in the diet of broilers, leads to flare-up of *C. perfringens* and NE [38,4].

Based on the latest proposed toxinotyping scheme *C. perfringens* strains are divided into toxinotypes A to G, Intestinal diseases including NE in poultry are associated with toxinotype G that produce NetB toxin [39]. The acute NE form can lead to overall mortality rates of 10 to 40% in birds within an affected flock. However, the subclinical form of the disease can affect a greater number of birds with intestinal damage, reduced weight gain, and decreased feed conversion efficiency [28].

The current approach for NE management entails elimination of infected flocks to prevent disease spread or administration of in-feed antibiotics as growth promoters that also controls *C. perferingens*. However, the addition of any antibiotic in feed is significantly limited because of concerns related to the emergence of the antibiotic resistant strains. Hence, attempts to vaccinate chickens as an alternative strategy has focused on the use of live microbes or inactivated toxins [3, 19, 20, 22].

Until recently, pathogenesis in NE was largely attributed to alpha-toxin, a phospholipase C, as an important virulence factor. This protein is contained two domains, the N-terminal and C-terminal domains. The N-terminal domain has hemolytic activity, while C-terminal domain involved in recognition and interaction with membrane phospholipids. The C-terminal domain of alpha-toxin is non-toxic [47, 32, 53]. Accordingly, vaccine development against NE in broilers were focused on recombinant C-terminal domain of alpha-toxin that was resulted in protection against NE in chicken [23, 55, 53].

More recent studies have demonstrated that alpha-toxin is not the major toxin associated with intestinal lesions. Keyburn et al. discovered that an alpha-toxin null mutant of the bacteria induced gastrointestinal necrotic lesion in chickens. Later, a novel toxin, pore forming protein termed necrotic enteritis toxin B-like (NetB) protein showed to destabilize target cell membrane and induces cell lysis [5,17,42],hence NetB has been considered as a critical virulence factor. There are three main domains in NetB including β-sandwich, stem and rim. The rim domains confers binding to target cell membrane, stem involved in penetration of toxin into the membrane and β-sandwich forms the protein backbone and oligomerize the heptameric structure of toxin [10]. Before pore formation, monomer structure of NetB should be oligomerised [17, 42]. It is demonstrated that site direct mutagenesis in the rim region of the NetB resulted in inability of the NetB to toxin oligomerisation and NetB toxicity [10, 42, 52].

More studies showed that other secreted proteins of virulent *C. perfringens* also interacted with bird's sera following infection [16, 26, 24].

Zinc metallopeptidase (Zmp), previously named hypothetical protein by Kulkarni et al., is another virulence factor that provides significant protection against sever *C. perferingens* challenge [22, 23, 24]. Epitope mapping of Zmp has revealed immunodominant epitopes that were defined as reactive peptides [24]. The peptidase catalytic activity and x-ray crystallographic structure of Zinc metallopeptidase, demonstrated that the ZMP domain anchors the host cell

surface and targets the host glycoprotein. It enables access to the underlying cells of mucus which results in degradation of the host epithelial cells [31, 33]. Therefore, Zmp has been proposed to be an important candidate for ameliorating protection against NE [22-24]. Several recent report have suggested that recombinant toxins, toxin derivatives, non-toxin variants, toxoids, or their combinations had led to variable level of protection [5, 14, 16, 18].

Previously the C-terminal domain of alpha toxin (CPA), and nontoxic variant of NetB were tested as vaccine candidates which showed a partial protection against NE in poultry [10, 18, 20]. However, immunization with a combination of CPA antigens and non-toxic variant of NetB induced complete protection against mild challenge and only partial protection in severe in-feed challenge [9].

In this study, we have expanded approach to combine the immunogenic regions of the desired toxins as a single fusion protein. We designed a novel trivalent fusion gene, NAM that encompasses protein domains of Alpha toxin, NetB, and ZMP predicted to be involved in NE pathogenesis caused by *Clostridium perfringens*. The fusion gene encode the C-terminal of alpha-toxin depleted of phospholipase activity, the rim and stem regions of NetB impaired in heptameric structure oligomerisation and the truncated form of metallopeptidase contained the reactive peptides. We employed an effective design strategy by selecting and combining highly immunogenic regions using combination of bioinformatics tools including ABCpred, Discotop and Vaxigen server. To confirm native folding of these main toxins we have used circular dichroism (CD) on the purified fusion protein.

Further, we demonstrated that the designed chimeric protein was highly immunogenic such that the antisera was able to detect and neutralizes the toxicity of crude extracellular toxins isolated from *C. perfringens*, using a cytotoxicity assay. The chimeric protein could be an effective subunit vaccine to prevent NE disease in poultries, however further filed studies need to be carried out to further confirm its application as a vaccine.

2. Materials and methods

2.1. Design and construction of recombinant NAM expression vector

Specific sequences from alpha-toxin (UniProtKB accession number P0C216), NetB (UniProtKB accession number C8XTG4) and a metallopeptidase protein (UniProtkB accession number Q8XKW1) were used to construct rNAM construct for expression in *E. coli*. Different

parameters including antigenicity, functional domains and hydrophobicity were involved in domain selection and order of the antigenic domains in the fusion construct. Six different arrangements of the three selected protein fragments were designed. The selected fragments were fused using two identical alpha-helix forming linkers $A(EAAAK)_4A$. According to multiple cloning sites in pET-28a vector (Novagen), for subcloning EcoRI and HindIII restriction sites were inserted in 5′ ad 3′ end of construct (Fig. 1). Moreover, each of subunits was cloned same as NAM.

2.2. Prediction of B cell epitopes and antigenicity

Linear B-cell epitopes in the full length primary protein sequences were predicted by ABCpred (http://crdd.osdd.net/raghava//abcpred/) and BepiPred (http://www.cbs.dtu.dk/services/BepiPred/), respectively [15,41]. Also, Discotope 2.0 server (http://www.cbs.dtu.dk/services/DiscoTope/) and Ellipro (http://tools.iedb.org/ellipro/) were used to determine conformational B-cell epitopes from 3D structure of fusion protein [21, 35]. The antigenicity of the selected protein fragments and fusion protein were evaluated using the VAXIJEN server (http://www.ddg-pharmfac.net/vaxijen/VaxiJen/VaxiJen.html) [8].

2.3. Analysis of primary structure

The ProtParam online tool (http://expasy.org/tools/protparam.html) was used for prediction of the physicochemical parameters, including molecular weight, theoretical isoelectric point (pI), total number of positive and negative residues, half-life, instability index, aliphatic index and grand average of hydropathicity (GRAVY). Moreover, functional domains of protein sequences were determined by means of the Expasy web server. The solubility of fusion protein was estimated using a web-based service available at the Oklahoma University web site (http://biotech.ou.edu/) [7]. All possible tertiary combinations were analyzed by I-TASSER server (https://zhanglab.ccmb.med.umich.edu/I-TASSER/) [57]. The analysis and visualization of the structures was performed by Accelrys Discovery Studio software (Accelrys, San Diego, CA, USA). To assess the validation of the predicted models, the model with the best tertiary structure in which all protein residues were exposed and had a significant score were selected and further evaluated by ProsA web server (https://prosa.services. came.sbg.ac.at/prosa) [51]. In addition, stoichiometry results of improved model of the fusion protein were assessed by

Ramachandran plot via PROCHECK server (https://www.ebi.ac.uk/thornton-srv/software/PROCHECK/) [25].

2.4. mRNA structure analysis

RNA secondary structure of the designed fusion constructs were evaluated by mfold web server (http://unafold.rna.albany.edu/?q=mfold) [58]. Efficiency of translation was analyzed based on structural stability and Gibbs free energy (ΔG).

2.5. Construction of expression vector

A fusion construct was synthesized (Biomatik Canada). Using two forward primer (FP1) 5′ ATAGAgaattcATGGTTTCTAATTCAATCGGA 3′ and reverse primer (RP1) 5′ CATAAaagcttTTACTCTTCACCCAAAGCAA 3′ (restriction sites in lower case) the two. EcoRI and HindIII restriction sites were added to the 5' and 3' end of the rNAM sequence using PCR. The amplified sequence was cloned into PET28a downstream of polyhistidin tag using the above restriction enzymes. The PET-NAM expression vector was transformed into E. coli strain BL21 (DE3) and later the integrity of rNAM was verified by sequencing technique (Bioneer, Korea).

2.6. Expression of fusion protein(s)

Expression of rNAM fusion protein and their subunits was induced by 1mM IPTG for 5 h at 37 °C. Bacterial cells were pelleted and resuspended in lysis buffer containing 100mM sodium phosphate buffer, PH: 8, 10mM Tris, 0.05% Tween 20. Then it sonicated on ice (5× 20 s with 20 s pause at amplitude 60) following centrifugation supernatant was stored at -20ºC and the protein expression yield was confirmed on SDS-page.

2.7. Protein purification

Fusion protein purification was performed by Ni-NTA affinity chromatography (QIAGEN Inc., USA). Overnight bacterial cultures were diluted 100-fold in fresh LB. Then cultures were induced to an optimal density (600nm) of 0.8 at 20°C with 0.6mM IPTG with shaking at 100 rpm for 6h. Bacterial cultures were harvested as described above. In order to harvest the produced proteins in soluble and inclusion body, we utilized two purification methods of native and denaturing conditions. The induced cell pellets were resuspended either in lysis buffer containing 50 mM sodium phosphate buffer (pH: 8), 2M NaCl, 10 mM imidazole, 1mM PMSF, 0.1 % v/v Tween 20 (native condition) or buffer containing above-mentioned ingredients with urea at 8M (denaturing condition). Then samples were sonicated on ice and centrifuged as mentioned in

previous section. The soluble part of supernatant containing 6 His-tagged fusion protein was incubated with nickel beads at 4°C for 1 h with mild agitation. The beads that were bound to 6-His tagged rNAM protein were resuspended in washing buffers 1-4, wash buffers 1,2 including 50 mM NaH2po4(PH:8), 2M NaCl, 30 mM imidazole, 0.1 % Tween20 and 1 % Triton X-100, , wash 3 and 4 same as wash 1,2 without Tween-20 and Triton X-100, containing 20 mM imidazole. Finally recombinant protein was eluted in elution buffer containing 50 mM NaH2po4 (PH: 8), 300mM NaCl, 300 mM imidazole and dialyzed against NaCl at 4°C. The quality and quantity of the purified recombinant protein was investigated using 10% SDS-PAGE and Bradford assay with BSA as a standard, respectively.

2.8. Immunization of rabbit, raising antibody and evaluation of IgG antibody responses to rNAM

Purified rNAM in PBS (pH 7.2) was used as antigen for immunization a New Zealand white rabbit (Pasteur Institute). On day zero, a pre-immune serum was collected and served as control. On day 1, 0.4 mg of rNAM protein as an emulsion in Complete Freund's Adjuvant was injected subcutaneously followed by two more injections on days 14 and 28 using a mixture of 0.25 mg rNAM with Incomplete Freund's Adjuvant via the same route. Blood samples were collected on day 42. Antibody level of the serum was monitored by indirect ELISA as described [1]. In brief, 96 well microtiter plates were coated with 0.5 µg of purified rNAM protein in carbonate-bicarbonate coating buffer (PH: 9.7) and incubated at 4°C overnight. The plates were washed with PBS containing 0.05 % Tween-20 (PBST) and blocked with PBST containing 5 % skimmed milk at 37°C for 1 hour. Two folds dilution of serum (1/500 to 1/65,536,000) in PBST containing 1% BSA were applied to the wells and incubated with mild agitation at 37°C for 1 hour and washed with PBST. A horseradish-peroxidase-conjugated Goat-anti rabbit IgG antibody (1:10,000) (BETHYL) were then added and incubated at 37°C for 1 hour. After washing, color was developed by addition of the 3,3′,5,5′-tetramethylbenzidine (TMB) and incubated at the room temperature for 15 min. Finally, absorbance at 450 nm was measured using microplate reader BioTek. Antibody titers were calculated at the highest serum dilution giving an OD 450 ≥ 0.4. All animal experiments were conducted in accordance with guidelines animal ethical committee with an ethical code IR.NIGEB.EC.1397.11.30 F from_National Institute of Genetic Engineering and Biotechnology.

2.9. Western blot analysis

Crude supernatant of recombinant bacterial culture containing rNAM fusion protein as well as its individual subunits were resolved by SDS-PAGE, transferred onto nitrocellulose membrane and blocked with phosphate-buffered saline (PBS) containing 3 % (w/v) BSA for 1 h. The membrane was then incubated with polyclonal anti-rNAM antibody at 1:10000 dilution (for alpha-toxin, Net B and ZMP) or monoclonal Anti-6X His tag antibody (Abcam18184, US) at1:3500 dilution (for rNAM) in PBST(PBS containing 1 % Tween 20) by gentle shaking at 4°C overnight. Following three washes with PBST, membrane was incubated with peroxidase-conjugated goat anti-mouse IgG (Sigma) and goat anti-rabbit IgG (Bethyl, USA) as secondary antibody diluted 1:5000 and 1:10000 in PBST for 1 h, respectively h. After washing with PBST, staining was developed using diaminobenzidine (1mg/ml) and H2O2 (o.3 µl/ml) (DAB substrate system, sigma-Aldrich, USA).

2.10. Analysis of the secondary structure of the designed fusion protein using Circular Dichroism

Far UV circular dichroism (CD) spectroscopy was used to characterize the secondary structure content and folding properties of fusion protein rNAM at room temperature using a JASCO J-810 Spectropolarimeter (Japan, Tokyo). The obtained spectra estimate the changes in secondary structure between two different purification methods. The samples were prepared with a concentration of 0.5 mg purified protein per ml, in 5 mM NaCl buffer. The prepared samples injected to the quartz cuvette with path length 1 mm, the far-UV region (250-190) and scanning speed of 200 nm/min. data quantification and comparison were carried out by the CDpro software (https://sites.bmb.colostate.edu/sreeram/CDPro/).

2.11. Cytotoxicity assay

The chicken hepatoma cell line (LMH, ATCC CRL-2117 Pasteur Institute (IRAN),) was grown in Waymouth's complete media (90% Waymouth's MB 752/1 (Invitrogen) supplemented with 10 % fetal bovine serum, L-glutamine, 100 U/ml penicillin and 100 µg/ml streptomycin). LMH cells were incubated in a humidified environment of 5% CO2 at 37ºC. For cytotoxicity assay, 96 well plates (SPL, Korea) were seeded with 5×10^3 LMH cells/well and incubated until almost 100% confluent. *C. perfringens* strains were a field isolates from NE-positive case of broiler flocks in Mashhad, Iran (kindly gifted by Dr. Razmyar, Ferdowsi university) [36, 37]. Among sixty *C. perfringens* strains isolated from infected cases in poultry farms, finally three *C.*

perfringens strains were selected. The strains with a desired secreted toxins selected based on PCR by designing specific primers to detect each toxin. Meanwhile the presence of toxins in each strain was further confirmed by western blot analysis using specific polyclonal anti-NAM antibody was capable of detecting the targeted toxins (data not shown).

Based on the fact that the Cp58 strain expressed all the three desired toxins (alpha toxin, NetB and metallopeptidase) and had the most toxic effects on LMH cell line, it was selected in subsequent studies.

A single colony of Cp58 strain grown on blood agar (Gibco) was inoculated in 5ml TPG broth (5% (w/v) BactoTrypton, 0.5 % (w/v) protease peptone, 0.4 % (w/v) glucose, 0.1 % (w/v) sodium thioglycolate) [27], and after growing anaerobically overnight at 37ºC, the cp58 was subcultured into 10 ml TPG to an OD_{600} of 0.6-0.8. The culture supernatant was obtained by centrifugation at 10000g for 20 min and filter sterilized through a 0.22 µm filter (Millipore). The filtrated crude toxin was diluted in two-fold dilution series, up to (a dilution of) 1:128(v/v) and added to LMH medium in triplicate and incubated for up to 18 h at 37ºC with 5 % CO2. The cells treated with 1% Triton X-100 and medium without cells were considered as positive and negative control, respectively. The conventional MTT assay were used for evaluating cell viability. After incubation, MTT solution with final concentration 1 mg/ml was added to LMH cells and incubated for 4 h. The precipitated dark blue formazan crystals in viable cells were solubilized with acidified isopropanol. Subsequently, after 10 min absorbance at 570 nm was measured in a microplate reader BioTek (BioTek Instruments Inc, Winooski, VT, USA). The results expressed as percentage of cytotoxicity.

2.12. Neutralization assay

The ability of the raised antisera obtained from rabbit was assessed to neutralize the toxicity of the crude toxin by an *in vitro* neutralization assay. LD50 was used as a parameter for the estimation of toxin potency in *C. perfringens* culture filtrates. The smallest amount of crude toxins that cause 50% lethality of LMH was defined as LD50 (lethal dose). The LD50 units of the crude toxin was incubated with antisera raised against rNAM at a series of final dilution 1:4, 1:8, 1:16 and 1:32 in cell culture medium for 1 h at 37 ºC. After incubation, the mixture was added to 96-well plate containing LMH cells as was mentioned in the cytotoxicity assay. Subsequently, the plate incubated and treated as mentioned above. Pre-immune sera and crude toxin were used as controls. All experiments were performed in triplicate.

3. Results

3.1. Designing of a fusion trivalent protein and *in silico* analysis of immunogenic properties

The order of protein domains in the fusion construct leading to a proper conformation for immunogenicity was determined by measuring the antigenicity index and analysis of predicted secondary and tertiary structures of possible combination of the domains in the fusion proteins. The antigenicity index of each selected fragments alone and in 6 possible orders in the fusion proteins were evaluated by VaxiJen. All combinations resulted in antigenicity index of 0.68 to 0.7 (threshold=0.4, ACC output), therefore, all arrangements were predicted to be antigenic. The conformational impact of different orders of the fragments in the constructs were analyzed by secondary structure prediction server (PORTER) and I-TASSER server for tertiary structure prediction. Finally, the highest similarity of secondary and tertiary structure of protein domains in the fusion construct to the native proteins was determined to be NetB- alpha toxin-ZMP (NAM). The three selected fragments were separated by two hydrophobic α-helix linkers $A(EAAAk)_4A$ which provide proper flexibility between functional domains.

3.2. Prediction of secondary and tertiary structure and determining structural validity

The accuracy of the predicted secondary structures was evaluated using reference structure of alpha-toxin, Net B and metallopeptidase in protein database (PDB). The results obtained by different algorithm showed that the PORTER server had the best secondary structure prediction of native and fusion proteins (Table 1). According to prediction of the PORTER server the rNAM chimeric protein composed of 18.59% alpha helix, 31.83% extended strand and 49.20% other forms, which showed 96.98%, 81.61% and 100 % residue identity in comparison to the native proteins prediction for ZMP, Net B and alpha toxin, respectively. The secondary structure prediction of fusion protein is illustrated in Figure 2A, as expected the α-helix linkers could link and separate the three fragments.

Tertiary structure Prediction of the fusion protein was performed by I-TASSER server. The best model was estimated by predicted confidence score (C score is typically in the range of -5 to 2) and appropriate exposure of each domain in 3D model. The C-score, TM (template modeling) and RMSD (root-mean square deviation) were -0.42, 0.66±0.13 and 8.9±4.6 A°, respectively. The accuracy of the model that predicted by ITASSER is estimated based on TM and RMSD when their native structure is known. Further analysis for structure refinement and validity was carried out by ProsA web and Ramachandran plot. The ProsA web results were expressed as z-

score. The z-score for the best predicted 3D model was -5.22 that is within the range of scores typically found for native proteins of similar size. As seen in Figure 2B the z-score plot indicates overall predicted model quality. Ramachandran plot analysis revealed that 85% of the residues located in the most favored regions, 11.6 % additionally allowed regions, 1.3 % generously allowed regions and 1.2 % disallowed regions (Fig 2C).

3.3. Physico-chemical parameters

Based on ProtParam analysis results, the molecular weight of the fusion protein was estimated to be 78 KD. The higher content residues with negatively charged than positively charged residues indicated that the isoelectric point of protein was in the acidic range (5.49). The extinction coefficient of the fusion protein at 280 nm was 118,150 $M^{-1}cm^{-1}$. The estimated half-life of fusion protein was more than 10 hours in different expression host. The instability index 20.47 indicated that the fusion protein classified as a stable protein. Thermostability of the fusion protein which defined as aliphatic index was 69.98. The GRAVY index of -0.65 showed that the fusion protein was soluble in water. Moreover, the solubility value of the fusion protein, using the web-based service of Oklahoma University, during expression in *E. coli* was 90.2%.

3.4. Identification of B-cell epitopes

A collection of linear and conformational B-cell epitopes of rNAM was created using various software. ABCpred software, a method based on artificial neural network [41], predicted 61 linear epitopes above the threshold value of 0.58 (Table S1). Additional 21 linear epitopes were predicted by BepiPred software based on combination of hidden Markov model and amino acid propensity scales (Table S2).

Moreover, the prediction of the possible conformational B-cell epitopes of the best 3D selected model was undertaken by DiscoTope 2.0 and Ellipro servers. DiscoTop 2.0 utilizes a combination of spatial neighborhood and half-sphere exposure which previously defined as sum propensity scores and contact number, respectively. The DiscoTop server predicted a total of 172 discontinuous B-cell epitope residues in 36 exposed regions at threshold -1 (Table S3). Furthermore, Ellipro server predicted 10 sets of discontinuous B-cell epitopes based on Thornton′s propensities and a residue clustering algorithm. The scores of antigenic regions and visualization of the rNAM discontinuous epitopes using Jmol is represented in table S4 and figure S6, respectively

3.5. mRNA structure validation

The stability of RNA secondary structure was evaluated by mfold web server. The comparison of thermodynamic features between optimized and un-optimized mRNA secondary structure indicated that the codon optimization significantly increased the stability of RNA structure, ΔG:-515.20 kcal/mol vs. ΔG: 466 kcal/mol. I addition, there were no hairpin or pseudoknot structure at the 5' terminus of the both RNA secondary structure (Fig. S5).

3.6. Testing immunoreactivity of the recombinant Net B, Alpha- toxin, ZMP, and rNAM with anti-NAM antibody

Whole bacterial cell lysates was prepared and the extracted rNAM protein was subjected to SDS-PAGE and a 78 kD band corresponding to rNAM was detected on the gel (Fig. 3). The blots was developed with a rabbit anti-NAM antibody in which protein bands of 78, 21, 14 and 37 kD corresponding to the size of expressed recombinant NAM, and individual recombinant proteins of Net B, Alpha- toxin and ZMP were immunoreactive with anti-NAM antibody. The soluble and inclusion body forms of rNAM protein was subjected to purification by Ni-NTA affinity chromatography (Fig. 4) and resulted in a target band with molecular weight of 78 kD.

3.7. Analysis of secondary structure of rNAM chimeric protein

In order to assess the correct folding of rNAM purified under native and also denaturing conditions followed by refolding of denatured protein on the column, the changes in secondary structure of the purified proteins were analyzed using CD spectroscopy (Fig. 5). In visual assessment changes in mean residual elipticity values at different wavelength supposed that the contents of α-helix, β-sheet and other secondary structural elements were slightly changed. CD spectrums have negative bands at 210 nm and 220 nm indicating the presence of both α-helix and β-sheet in the structure of rNAM. In-situ refolding of denatured rNAM on the column resulted in 9.2 % decrease in β-sheet, 3.4 % increase in α-helix and 6.12 % increase in random coil. The Far-UV spectrum of rNAM protein exhibited that the purified rNAM under native condition was properly folded and is more compatible with the predicted secondary structure of the original proteins.

3.8. Immune response to rNAM

The level of IgG antibody against rNAM protein in the rabbit sera was measured by ELISA using the purified rNAM protein as an antigen. The control serum has shown no background in

the levels of anti NAM-IgG antibody titer (fig.6). The average IgG titer of the serum against rNAM reached to 1:8192000 following three boosts of rNAM protein.

3.9. Cytotoxicity against crude clostridium toxins

To quantify the cytotoxicity effects of the pathogenic field strain Cp58, several dilutions of *C. perfringens* culture supernatant were tested on the LMH cells. The results showed that the media containing the crude toxins had significant toxicity on LMH, with the dilution of 1:8 leading to approximately 50% of the LMH cell death (Figure 7). This was set as a reference dilution to determine neutralization of toxicity in the presence of anti-rNAM sera.

3.10. In vitro neutralization assay

After determination of the LD50 of Cp58 toxin activity of culture supernatant on LMH cells, the ability of the antisera raised against chimeric rNAM antigen to protect against the crude toxin was estimated by in vitro toxin neutralization assay. Fig 8 illustrates morphological effects of Cp58 crude toxins on LMH cells. Untreated cells in left panel show the epithelial and dendritic-like growth. Pre incubation with 2× LD50 crud toxins with the antisera raised against rNAM chimeric protein at the 1:4 dilution, neutralized Cp58 toxins and resulted in only 6.06 % cell death while pre incubation with pre-immune sera did not neutralize toxins and caused cell blebbing and swelling (resulted in 92% cell death). This observation revealed that the anti rNAM sera was able to efficiently neutralize the toxin activity *in vitro* (Fig. 8)

4. Discussion

Necrotic enteritis (NE) is one of the most common diseases affecting poultry with sudden increase in the flock mortality at about 3 to 4 weeks of age coinciding with a drop in the maternal antibody levels in growing chickens [30,48]. In recent years, efforts have been concentrated on developing novel recombinant vaccines to protect against NE outbreaks caused by *C. perferingens*. Attempts to produce efficient vaccines have faced major limitations, due to some safety concerns in vaccination with active toxins at commercial settings and difficulty in balancing between attenuation without losing protection for inactivated toxins [29, 30]. Therefore, a combination of immunogenic segments of several important toxins for preventing NE pathology might be an effective and safe approach to provide protection against *C. perfringens*. Here, we constructed a fusion protein that is composed of immunogenic fragments of three toxins called rNAM, fusion protein, consisted of a 114 residue fragment from the C-terminus of alpha toxin, 117 residues from the C-terminus of NetB, and a truncated Zinc

metallopeptidase protein. The carboxy terminus fragment from alpha-toxin is the region responsible for membrane recognition and binding with no phospholipase C activity which is associated to the N-terminus region of the protein [32]. Previous studies have shown a strong immune response and protection against hemolysis after exposure to *C. perfringens* toxins in chickens injected with the C-terminal domain of alpha-toxin which suggest that this domain is sufficient to provide immunity [46]. Furthermore, a 177 residue fragment from NetB protein was chosen due to its immunogenic properties lacking the ability to oligomerise into heptameric structure and to form transmembrane β-barrel essential for its toxicity [10]. The alpha toxin and NetB protein fragments were linked to a truncated form of ZMP toxin containing its metallopeptidase domain associated with strongly reactive antigenic peptide. The ZMP has been confirmed to be responsible for adhesion to the host membrane and degradation of proteins [24, 31]. The functional protein domains in rNAM were linked together using two alpha helical hydrophobic linkers. The predicted 3D structure showed three domains in the fusion protein were properly separated through two repeats of the linkers between NetB, alpha-toxin and ZMP as we have reported in previous studies [1, 40].

For comparison of the results of secondary structure prediction by different servers and evaluate its validity, the PORTER program has predicted closest similarity of secondary structure of the protein domains in the chimeric proteins to their native counterparts (Table 1).

The DiscoTop server predicted 166 conformational epitopes present over the full sequence of the fusion protein (Table S3). Out of that, 54.81%, 20.12% and 25.6% of the total number of conformational epitopes were found in the NetB region, alpha-toxin and ZMP regions, respectively. Accordingly, as predicted by Ellipro server, NetB domain contained a higher number of conformational epitopes with the highest score than alpha-toxin and ZMP which further confirm the DiscoTop server prediction results. Therefore, the sequences which have the most overlap regions have been chosen.

The available epitopes in the fusion protein may differ after fusion due to inevitable changes in the whole protein structure and folding, resulting in loss or creation of new epitopes [40, 54]. Thus, among the six different arrangements, we selected the one with the least changes around the linkers based on PORTER prediction. As expected, using BepiPred and ABCpred servers, the linker sequences were not distinguished as conformational epitopes.

According to the C-score the rNAM model signified as a model with high confidence comparing to the other 6 combinations of these peptides the template modeling score and z-score indicated that this model has a correct topology as native structure, and Ramachandran plot predicted that the quality of the model is acceptable.

It is known that a significant portion (~ 90%) of the B-cells respond only to discontinuous and highly conformational epitopes. Therefore, to elicit better immunogenicity it is crucial to keep the proper confirmation of the epitopes in the fusion protein structure [11, 34]. Moreover, the previous studies demonstrated that conformational epitopes of alpha toxin are more potent than liner epitopes with potential to be applied as a vaccine to elicit immune response and protection against NE [23, 24]. To address the above concerns, based on tertiary structure, the rNAM fusion protein were exposed to the environment and showed that is suitable to be used as candidate vaccine as it is highly immunogenic.

According to secondary structure analysis through CD, the purified protein under native condition was correctly folded compared to the original proteins. However, because of the yield there is a need for refolding of produced inclusion bodies. In many cases, refolding of denatured form of the recombinant proteins into native conformation is cumbersome and reduction of alpha-helix and β-sheet in renatured protein is inevitable and denaturation is mostly irreversible [2, 44, 45]. To evaluate the effect of different purification conditions and refolding on the column process on conformation of rNAM, CD analysis was performed. Results showed that in the presence of urea in lysis buffer and following purification, the fusion protein retained almost properly folded structure. Therefore, the soluble and renature forms of rNAM protein were used for further analysis. Moreover, it has been reported in some cases that slightly changes in structural properties of the fusion protein compared to the native form induced no negative effects on immunoreactivity and potency characteristics of these proteins [12, 40].

This study showed that the chimeric rNAM protein was highly immunogenic and induced high titer of specific antibodies which showed strongly immunoreactivity with four *E.coli* expressed recombinant Net B, alpha-toxin, ZMP and rNAM as 21 kD, 14 kD, 34 kD and 78 kD protein bands in western blot analysis, respectively. These results not only provide direct evidence that the fusion protein are nontoxic at the doses used for vaccination, but also showed that raised antibody is able to recognize each of the toxins.

To date several toxins have been evaluated as suitable candidates for inducing protection against NE; among them alpha-toxin, NetB and recently, ZMP have been proposed as important virulence factors for *C. perfringens* [5,9,18,24]. In this study the immunogenic part of these three predominant toxins were fused to make a single chimeric protein and used to immunize rabbits to generate anti-sera against the toxins. Our chimeric protein proved to elicit a potent immune response and the anti-sera generated showed much stronger reaction against the toxins compared to previously report neutralizing antibodies. The reason for high neutralizing activity detected in the serum of the immunized rabbits might be the result of highly immunogenic epitopes present on the fusion protein used [43,44]. In our previous study a fusion immunogen, with a combination of parts of the three toxins of alpha-toxin, NetB and Tpel, was used to raise antisera which was resulted in strong neutralizion of the toxicity of native alpha-toxin [40].

In the present study the rNAM induced production of specific antisera that effectively neutralized 2× LD50 dose of crude toxin extract of *C. perfringens* resulting in a survival rate of 94% of LMH cells. Our study suggests that rNAM may potentially be used to vaccinate chickens to reduce toxicity of C. perfringens and the rate of NE outbreaks. Further in vivo studies in NE models will be necessary to show efficacy of rNAM.

Acknowledgments

This research was financially supported in part by grant No. 951106 of Biotechnology Development council of the Islamic Republic of Iran and Iran National Science Foundation by project No. 96006074. The authors would like to thank the Genetics and Agricultural Biotechnology Institute of Tabarestan (GABIT), Sari Agriculture Science and Natural Resource University (SANRU), National Institute of Genetic Engineering and Biotechnology (NIGEB) and Pasteur Institute of Iran for providing the necessary equipment. The authors thank Dr. Mirabzadeh (Pasture institute, IRAN) for her technical assistant.

References

[1] J. Amani, A.H. Salmanian, S. Rafati, S.L. Mousavi, Immunogenic properties of chimeric protein from espA, eae and tir genes of Escherichia coli O157: H7, Vaccine 28(42) (2010) 6923-6929.

[2] M.R. Arjomand, G. Ahmadian, M. Habibi-Rezaei, M. Hassanzadeh, A.A. Karkhane, A.A. Moosavi-Movahedi, M. Amanlou, The importance of the non-active site and non-periodical structure located histidine residue respect to the structure and function of exo-inulinase, International journal of biological macromolecules 98 (2017) 542-549.

[3] D.L. Caly, R. D'Inca, E. Auclair, D. Drider, Alternatives to Antibiotics to Prevent Necrotic Enteritis in Broiler Chickens: A Microbiologist's Perspective, Frontiers in microbiology 6 (2015).

[4] M.A. Chambers, S.P. Graham, R.M. La Ragione, Challenges in Veterinary Vaccine Development and Immunization, Vaccine Design: Methods and Protocols, Volume 2: Vaccines for Veterinary Diseases (2016) 3-35.
[5] S.P.F. da Costa, D. Mot, M. Bokori-Brown, C.G. Savva, A.K. Basak, F. Van Immerseel, R.W. Titball, Protection against avian necrotic enteritis after immunisation with NetB genetic or formaldehyde toxoids, Vaccine 31(37) (2013) 4003-4008.
[6] S. Das, S. Majumder, J.J. Kingston, H.V. Batra, Generation and characterization of recombinant bivalent fusion protein r-Cpib for immunotherapy against Clostridium perfringens beta and iota toxemia, Molecular immunology 70 (2016) 140-148.
[7] A.A. Diaz, E. Tomba, R. Lennarson, R. Richard, M.J. Bagajewicz, R.G. Harrison, Prediction of protein solubility in Escherichia coli using logistic regression, Biotechnology and bioengineering 105(2) (2010) 374-383.
[8] I.A. Doytchinova, D.R. Flower, VaxiJen: a server for prediction of protective antigens, tumour antigens and subunit vaccines, BMC bioinformatics 8(1) (2007) 4.
[9] S.P. Fernandes da Costa, D. Mot, S. Geeraerts, M. Bokori-Brown, F.V. Immerseel, R.W. Titball, Variable protection against experimental broiler necrotic enteritis after immunisation with the C-terminal fragment of Clostridium perfringens alpha-toxin and a non-toxic NetB variant, Avian Pathology (just-accepted) (2015) 1-26.
[10] S.P. Fernandes da Costa, C.G. Savva, M. Bokori-Brown, C.E. Naylor, D.S. Moss, A.K. Basak, R.W. Titball, Identification of a key residue for oligomerisation and pore-formation of Clostridium perfringens NetB, Toxins 6(3) (2014) 1049-1061.
[11] J.M. Gershoni, A. Roitburd-Berman, D.D. Siman-Tov, N.T. Freund, Y. Weiss, Epitope mapping, BioDrugs 21(3) (2007) 145-156.
[12] J.C. Gupta, R.S. Hada, P. Sahai, G. Talwar, Development of a novel recombinant LHRH fusion protein for therapy of androgen and estrogen dependent cancers, Protein expression and purification 134 (2017) 132-138.
[13] F.V. Immerseel, J.D. Buck, F. Pasmans, G. Huyghebaert, F. Haesebrouck, R. Ducatelle, Clostridium perfringens in poultry: an emerging threat for animal and public health, Avian pathology 33(6) (2004) 537-549.
[14] S.I. Jang, H.S. Lillehoj, S.-H. Lee, K.W. Lee, E.P. Lillehoj, Y.H. Hong, D.-J. An, W. Jeong, J.-E. Chun, F. Bertrand, Vaccination with Clostridium perfringens recombinant proteins in combination with Montanide™ ISA 71 VG adjuvant increases protection against experimental necrotic enteritis in commercial broiler chickens, Vaccine 30(36) (2012) 5401-5406.
[15] M.C. Jespersen, B. Peters, M. Nielsen, P. Marcatili, BepiPred-2.0: improving sequence-based B-cell epitope prediction using conformational epitopes, Nucleic acids research 45(W1) (2017) W24-W29.
[16] Y. Jiang, R.R. Kulkarni, V.R. Parreira, J.F. Prescott, Immunization of broiler chickens against Clostridium perfringens-induced necrotic enteritis using purified recombinant immunogenic proteins, Avian diseases 53(3) (2009) 409-415.
[17] A.L. Keyburn, J.D. Boyce, P. Vaz, T.L. Bannam, M.E. Ford, D. Parker, A. Di Rubbo, J.I. Rood, R.J. Moore, NetB, a new toxin that is associated with avian necrotic enteritis caused by Clostridium perfringens, PLoS pathog 4(2) (2008) e26.
[18] A.L. Keyburn, R.W. Portela, K. Sproat, M.E. Ford, T.L. Bannam, X. Yan, J.I. Rood, R.J. Moore, Vaccination with recombinant NetB toxin partially protects broiler chickens from necrotic enteritis, Vet Res 44 (2013) 54.
[19] A.L. Keyburn, S.A. Sheedy, M.E. Ford, M.M. Williamson, M.M. Awad, J.I. Rood, R.J. Moore, Alpha-toxin of Clostridium perfringens is not an essential virulence factor in necrotic enteritis in chickens, Infection and immunity 74(11) (2006) 6496-6500.
[20] A.L. Keyburn, X.-X. Yan, T.L. Bannam, F. Van Immerseel, J.I. Rood, R.J. Moore, Association between avian necrotic enteritis and Clostridium perfringens strains expressing NetB toxin, Veterinary research 41(2) (2010) 1-8.

[21] J.V. Kringelum, C. Lundegaard, O. Lund, M. Nielsen, Reliable B cell epitope predictions: impacts of method development and improved benchmarking, PLoS computational biology 8(12) (2012) e1002829.
[22] R. Kulkarni, V. Parreira, Y.-F. Jiang, J. Prescott, A live oral recombinant Salmonella enterica serovar Typhimurium vaccine expressing Clostridium perfringens antigens confers protection against necrotic enteritis in broiler chickens, Clinical and Vaccine Immunology 17(2) (2010) 205-214.
[23] R. Kulkarni, V. Parreira, S. Sharif, J. Prescott, Clostridium perfringens antigens recognized by broiler chickens immune to necrotic enteritis, Clinical and vaccine immunology 13(12) (2006) 1358-1362.
[24] R. Kulkarni, V. Parreira, S. Sharif, J. Prescott, Oral immunization of broiler chickens against necrotic enteritis with an attenuated Salmonella vaccine vector expressing Clostridium perfringens antigens, Vaccine 26(33) (2008) 4194-4203.
[25] R. Laskowski, M. MacArthur, J. Thornton, PROCHECK: validation of protein-structure coordinates, (2006).
[26] K. Lee, H.S. Lillehoj, G. Li, M.-S. Park, S.I. Jang, W. Jeong, H.-Y. Jeoung, D.-J. An, E.P. Lillehoj, Identification and cloning of two immunogenic Clostridium perfringens proteins, elongation factor Tu (EF-Tu) and pyruvate: ferredoxin oxidoreductase (PFO) of C. perfringens, Research in Veterinary Science 91(3) (2011) e80-e86.
[27] D. Leslie, N. Fairweather, D. Pickard, G. Dougan, M. Kehoe, Phospholipase C and haemolytic activities of Clostridium perfringens alpha-toxin cloned in Escherichia coli: sequence and homology with a Baciilus cereus phospholipase C, Molecular microbiology 3(3) (1989) 383-392.
[28] R. McDevitt, J. Brooker, T. Acamovic, N. Sparks, Necrotic enteritis; a continuing challenge for the poultry industry, World's Poultry Science Journal 62(2) (2006) 221-247.
[29] D. Mot, L. Timbermont, E. Delezie, F. Haesebrouck, R. Ducatelle, F. Van Immerseel, Day-of-hatch vaccination is not protective against necrotic enteritis in broiler chickens, Avian Pathology 42(2) (2013) 179-184.
[30] D. Mot, L. Timbermont, F. Haesebrouck, R. Ducatelle, F. Van Immerseel, Progress and problems in vaccination against necrotic enteritis in broiler chickens, Avian Pathology 43(4) (2014) 290-300.
[31] S. Nakjang, D.A. Ndeh, A. Wipat, D.N. Bolam, R.P. Hirt, A novel extracellular metallopeptidase domain shared by animal host-associated mutualistic and pathogenic microbes, PLoS One 7(1) (2012) e30287.
[32] C.E. Naylor, J.T. Eaton, A. Howells, N. Justin, D.S. Moss, R.W. Titball, A.K. Basak, Structure of the key toxin in gas gangrene, Nature Structural and Molecular Biology 5(8) (1998) 738.
[33] I. Noach, E. Ficko-Blean, B. Pluvinage, C. Stuart, M.L. Jenkins, D. Brochu, N. Buenbrazo, W. Wakarchuk, J.E. Burke, M. Gilbert, Recognition of protein-linked glycans as a determinant of peptidase activity, Proceedings of the National Academy of Sciences 114(5) (2017) E679-E688.
[34] A. Pomés, Relevant B cell epitopes in allergic disease, International archives of allergy and immunology 152(1) (2010) 1-11.
[35] J. Ponomarenko, H.-H. Bui, W. Li, N. Fusseder, P.E. Bourne, A. Sette, B. Peters, ElliPro: a new structure-based tool for the prediction of antibody epitopes, BMC bioinformatics 9(1) (2008) 514.
[36] J. Razmyar, G.A. Kalidari, A. Tolooe, M. Rad, A.R. Movassaghi, Genotyping of Clostridium perfringens isolated from healthy and diseased ostriches (Struthio camelus), Iranian journal of microbiology 6(1) (2014) 31.
[37] J. Razmyar, S.M. Peighambari, A.H. Zamani, Detection of a Newly Described Bacteriocin, Perfrin, Among C lostridium perfringens Isolates from Healthy and Diseased Ostriches and Broiler Chickens in Iran, Avian diseases 61(3) (2017) 387-390.
[38] N.J. Rodgers, R.A. Swick, M.S. Geier, R.J. Moore, M. Choct, S.-B. Wu, A multifactorial analysis of the extent to which Eimeria and fishmeal predispose broiler chickens to necrotic enteritis, Avian diseases 59(1) (2014) 38-45.
[39] J.I. Rood, V. Adams, J. Lacey, D. Lyras, B.A. McClane, S.B. Melville, R.J. Moore, M.R. Popoff, M.R. Sarker, J.G. Songer, Expansion of the Clostridium perfringens toxin-based typing scheme, Anaerobe 53 (2018) 5-10.

[40] A. Rostami, F. Goshadrou, R.P. Langroudi, S.Z. Bathaie, A. Riazi, J. Amani, G. Ahmadian, Design and expression of a chimeric vaccine candidate for avian necrotic enteritis, Protein Engineering, Design and Selection 30(1) (2016) 39-45.
[41] S. Saha, G. Raghava, Prediction of continuous B-cell epitopes in an antigen using recurrent neural network, Proteins: Structure, Function, and Bioinformatics 65(1) (2006) 40-48.
[42] C.G. Savva, S.P.F. da Costa, M. Bokori-Brown, C.E. Naylor, A.R. Cole, D.S. Moss, R.W. Titball, A.K. Basak, Molecular architecture and functional analysis of NetB, a pore-forming toxin from Clostridium perfringens, Journal of Biological Chemistry 288(5) (2013) 3512-3522.
[43] D. Shreya, S.R. Uppalapati, J.J. Kingston, M.H. Sripathy, H.V. Batra, Immunization with recombinant bivalent chimera r-Cpae confers protection against alpha toxin and enterotoxin of Clostridium perfringens type A in murine model, Molecular immunology 65(1) (2015) 51-57.
[44] S.M. Singh, A.K. Panda, Solubilization and refolding of bacterial inclusion body proteins, Journal of bioscience and bioengineering 99(4) (2005) 303-310.
[45] N. Sreerama, S.Y. Venyaminov, R.W. Woody, Estimation of protein secondary structure from circular dichroism spectra: inclusion of denatured proteins with native proteins in the analysis, Analytical biochemistry 287(2) (2000) 243-251.
[46] D.L. Stevens, R.W. Titball, M. Jepson, C.R. Bayer, S.M. Hayes-Schroer, A.E. Bryant, Immunization with the C-domain of α-toxin prevents lethal infection, localizes tissue injury, and promotes host response to challenge with Clostridium perfringens, Journal of Infectious Diseases 190(4) (2004) 767-773.
[47] R.W. Titball, C.E. Naylor, A.K. Basak, The Clostridium perfringensα-toxin, Anaerobe 5(2) (1999) 51-64.
[48] A. Ulmer-Franco, G. Cherian, N. Quezada, G. Fasenko, L. McMullen, Hatching egg and newly hatched chick yolk sac total IgY content at 3 broiler breeder flock ages, Poultry science 91(3) (2012) 758-764.
[49] F.A. Uzal, J.C. Freedman, A. Shrestha, J.R. Theoret, J. Garcia, M.M. Awad, V. Adams, R.J. Moore, J.I. Rood, B.A. McClane, Towards an understanding of the role of Clostridium perfringens toxins in human and animal disease, Future microbiology 9(3) (2014) 361-377.
[50] F. Van Immerseel, J.I. Rood, R.J. Moore, R.W. Titball, Rethinking our understanding of the pathogenesis of necrotic enteritis in chickens, Trends in microbiology 17(1) (2009) 32-36.
[51] M. Wiederstein, M.J. Sippl, ProSA-web: interactive web service for the recognition of errors in three-dimensional structures of proteins, Nucleic acids research 35(suppl_2) (2007) W407-W410.
[52] E. Williamson, R. Titball, A genetically engineered vaccine against the alpha-toxin of Clostridium perfringens protects mice against experimental gas gangrene, Vaccine 11(12) (1993) 1253-1258.
[53] X.-X. Yan, C.J. Porter, S.P. Hardy, D. Steer, A.I. Smith, N.S. Quinsey, V. Hughes, J.K. Cheung, A.L. Keyburn, M. Kaldhusdal, Structural and functional analysis of the pore-forming toxin NetB from Clostridium perfringens, MBio 4(1) (2013) e00019-13.
[54] N. Zeinalzadeh, A.H. Salmanian, G. Goujani, J. Amani, G. Ahangari, A. Akhavian, M. Jafari, A Chimeric protein of CFA/I, CS6 subunits and LTB/STa toxoid could protect immunized mice against enterotoxigenic Escherichia coli, Microbiology and immunology (2017).
[55] B. Zekarias, H. Mo, R. Curtiss, Recombinant attenuated Salmonella enterica serovar Typhimurium expressing the carboxy-terminal domain of alpha toxin from Clostridium perfringens induces protective responses against necrotic enteritis in chickens, Clinical and Vaccine Immunology 15(5) (2008) 805-816.
[56] J. Zeng, G. Deng, J. Wang, J. Zhou, X. Liu, Q. Xie, Y. Wang, Potential protective immunogenicity of recombinant Clostridium perfringens α–β2–β1 fusion toxin in mice, sows and cows, Vaccine 29(33) (2011) 5459-5466.
[57] Y. Zhang, I-TASSER server for protein 3D structure prediction, BMC bioinformatics 9(1) (2008) 40.
[58] M. Zuker, Mfold web server for nucleic acid folding and hybridization prediction, Nucleic acids research 31(13) (2003) 3406-3415.

Legends

Fig 1. The schematic representation of the recombinant construct containing three immunogen.

Fig. 2. Evaluation of the predicted (A) rNAM secondary structure by SOPMA, Two helix picks are represented two linkers, (B)Tertiary structure of fusion protein by proSA and (C) Ramachandran plot. (D) Prediction of tertiary structure by ITASSER, each domains are efficiently separated by two linkers.

Fig. 3. Western blot of (A) each selected immunogenic proteins α-toxin, NetB and ZMP were probed with anti-rNAM antibody and (B) detection of rNAM fusion protein using anti-His antibody.

Fig. 4. Expression and purification of rNAM fusion protein (PET28-NAM) as a candidate vaccine protein in *E.coli* cells by SDS-PAGE. Lane M: protein molecular weight marker; lane 1: uninduced; lane 2: induced *E.coli* cells bearing NAM-PET28 plasmid; lane 3: soluble part of supernatant containing NAM protein; lane 4: flow-through from column; lane 5, 6 and 7: wash 1, 2 and 3, respectively; lane 8 and 9: elution 1 and 2.

Fig. 5. Far-UV spectroscopy analysis to determine secondary structure content of rNAM protein under two purification methods. The secondary structure that revealed by CD was compared to predicted secondary structure by bioinformatics tools.

Fig 6. IgG antibody titration in rabbit against immunotoxin NAM. Rabbit was injected three times at interval two weeks with recombinant NAM protein. Pre-immune sera was used as control.

Fig 7. LMH cytotoxicity assay. Culture supernatant at several dilutions was prepared from field isolate cp58. Error bare depict standard deviation (SD). The amount of cytotoxicity induced by each dilution of crude toxin is expressed by average. The experiments were performed in triplicate.

Fig 8. Neutralization of *C. perfringens* supernatant. Several dilutions of pre-immune sera and antisera raised against rNAM were incubated with cp58 supernatant (2×LD 50) for 1 h at 37ºC. The concoction of toxin and sera were added to LMH cells, after 16 h incubation, cells viability was measured. (A) Cytopathic effects were expressed as percent of cytotoxicity. (B) Visually neutralization effects were illustrated, (a, c) negative control LMH cells before treatment, (b) crude toxin pretreated with pre-immune sera and (d) crude toxin pretreated with rabbit anti-NAM antisera. Cytopathic effects were visualized under a light microscope at 100 × magnification. The experiments were performed in triplicate and data are represented in mean ± S.D.

Figures and Tables

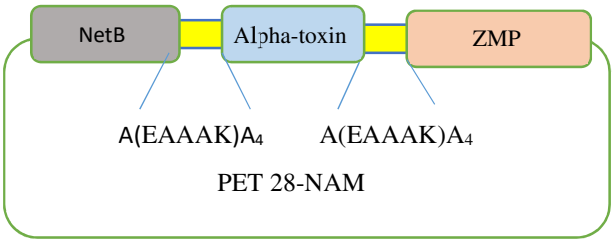

Fig 1. The schematic representation of the recombinant construct containing three immunogen.

Table 1. Secondary structure evaluation of proteins using different prediction servers.

Prediction model	Type of secondary structure	Protein		
		Alpha-toxin	Net B	ZMP
Native	Alpha helix	2.63	3.95	35.07
	Extended strand	48.24	56.49	16.9
	Random coil(other)	49.13	39.55	48.03
GOR IV	Alpha helix	18.24	10.17	22.46
	Extended strand	35.96	31.64	27.38
	Random coil	45.61	58.19	50.15
PORTER	Alpha helix	2.63	5.64	33.84
	Extended strand	49.12	54.8	16.3
	Random coil	48.25	39.54	49.84
DSSP	Alpha helix	2.6	2.3	31.4
	Extended strand	35.1	43.5	13.8
	Random coil(other)	62.3	54.2	54.8
SOPMA	Alpha helix	10.53	1.69	32.62
	Extended strand	37.72	35.59	19.38
	Random coil(other)	51.75	62.71	48

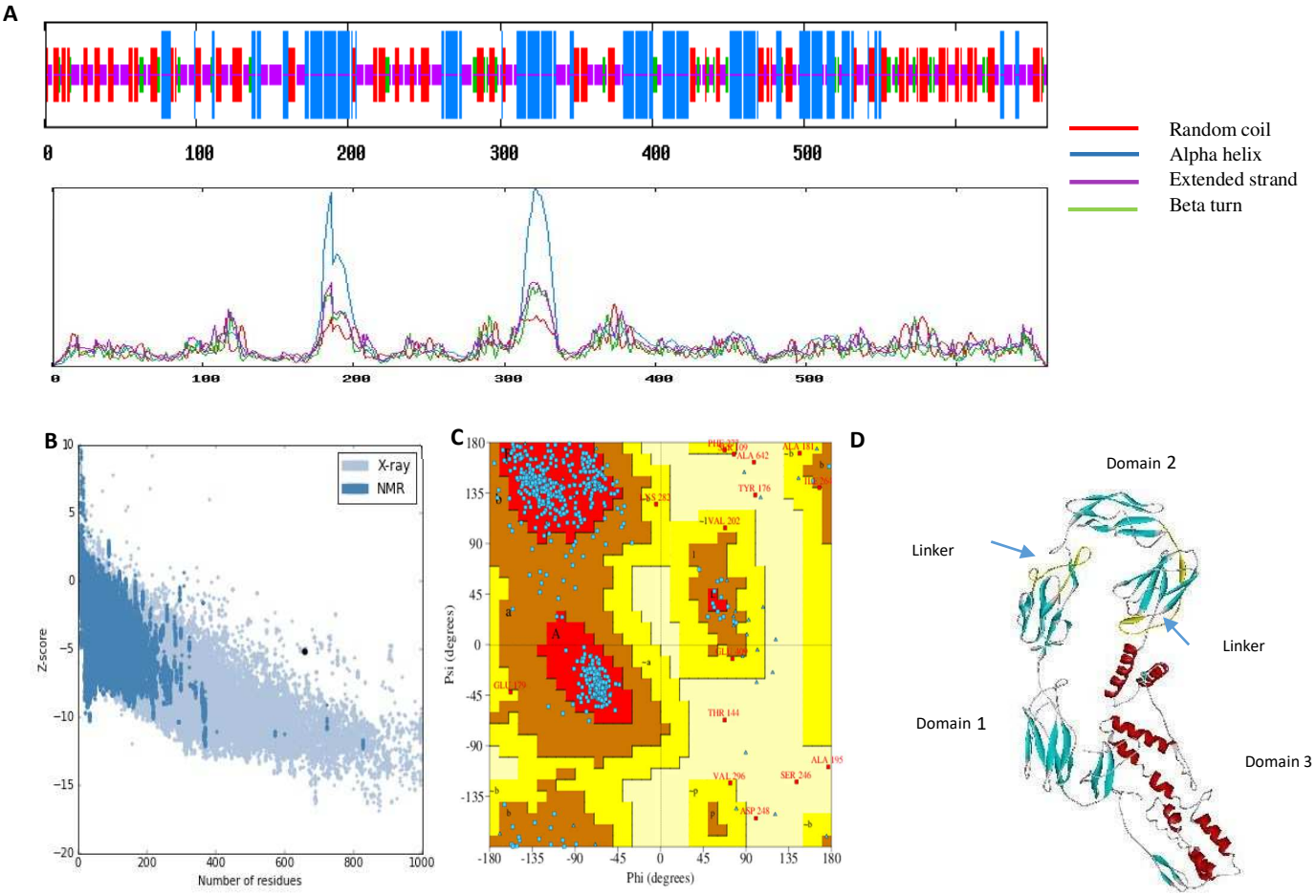

Fig. 2. Evaluation of the predicted (A) rNAM secondary structure by SOPMA, Two helix picks are represented two linkers, (B)Tertiary structure of fusion protein by proSA and (C) Ramachandran plot. (D) Prediction of tertiary structure by ITASSER, each domains are efficiently separated by two linkers.

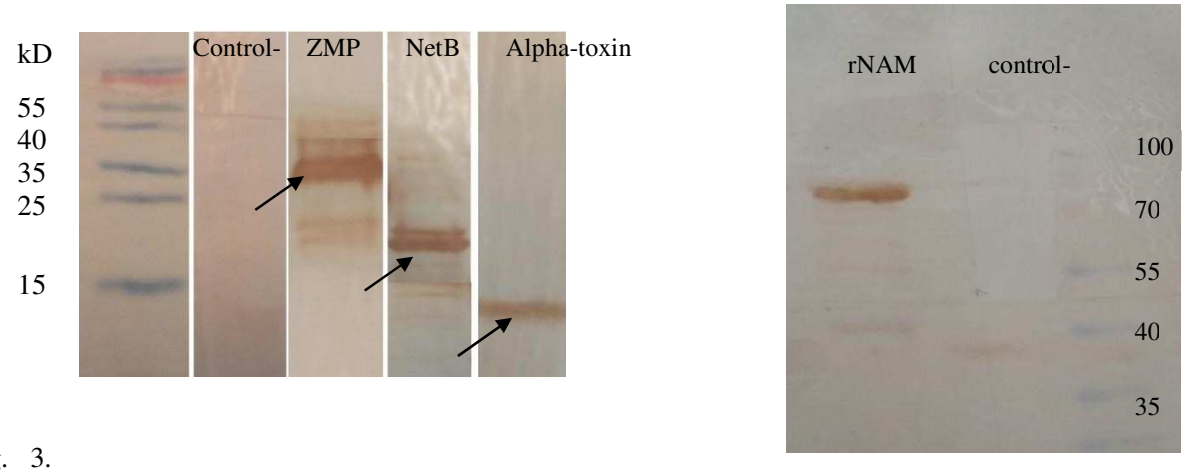

Fig. 3.

Western blot of (A) each selected immunogenic proteins α-toxin, NetB and ZMP reacted with rabbit anti-rNAM antibody and (B) detection of rNAM fusion protein using anti-His antibody.

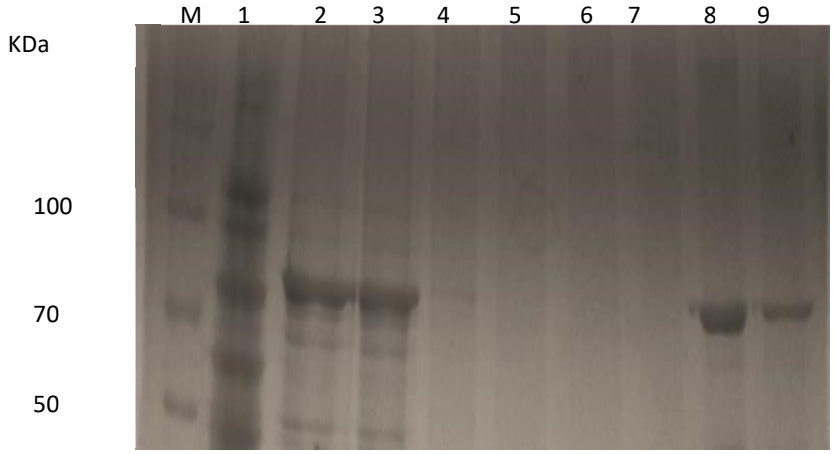

Fig. 4. Expression and purification of rNAM fusion protein (PET28-NAM) as a candidate vaccine protein in *E.coli* cells by SDS-PAGE. Lane M: protein molecular weight marker; lane 1: uninduced; lane 2: induced *E.coli* cells bearing NAM-PET28 plasmid; lane 3: soluble part of supernatant containing NAM protein; lane 4: flow-through from column; lane 5, 6 and 7: wash 1, 2 and 3, respectively; lane 8 and 9: elution 1 and 2.

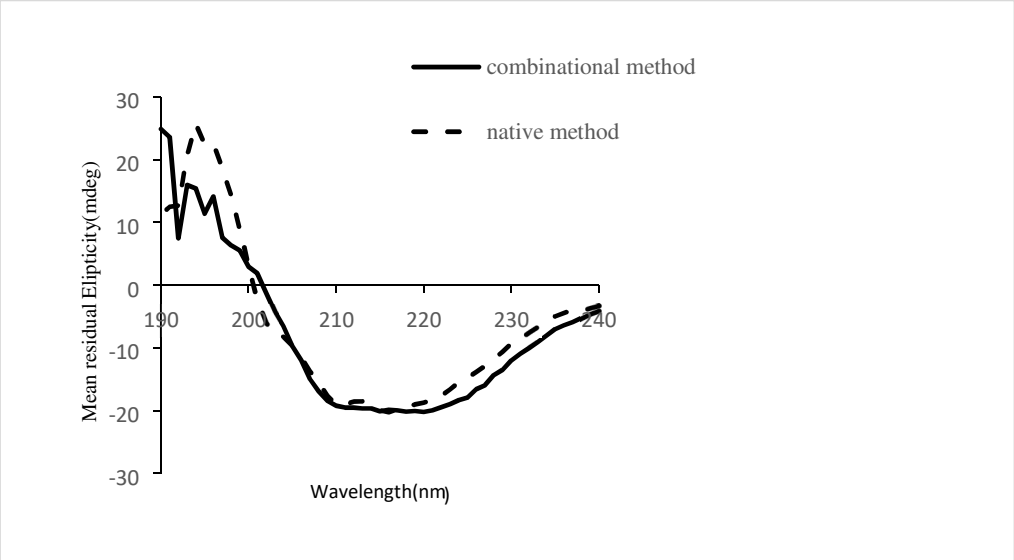

Secondary structure	Native form of Purified rNAM	Combination form of purified rNAM	Wild type(predicted)
Alpha-helix (%)	16.29	22.027	18.59
Beta sheet (%)	32.38	22.63	31.83
Random Coil (%)	51.33	55.32	49.20

Fig. 5. Far-UV spectroscopy analysis to determine secondary structure content of rNAM protein under two purification methods. The secondary structure that revealed by CD was compared to predicted secondary structure by bioinformatics tools.

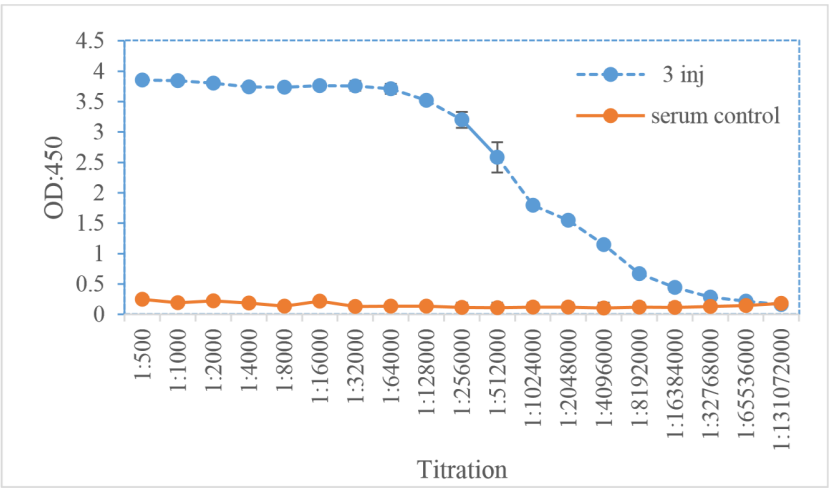

Fig 6. IgG antibody titration in rabbit against immunotoxin NAM. Rabbit was injected three times at interval two weeks with recombinant NAM protein. Pre-immune sera was used as control.

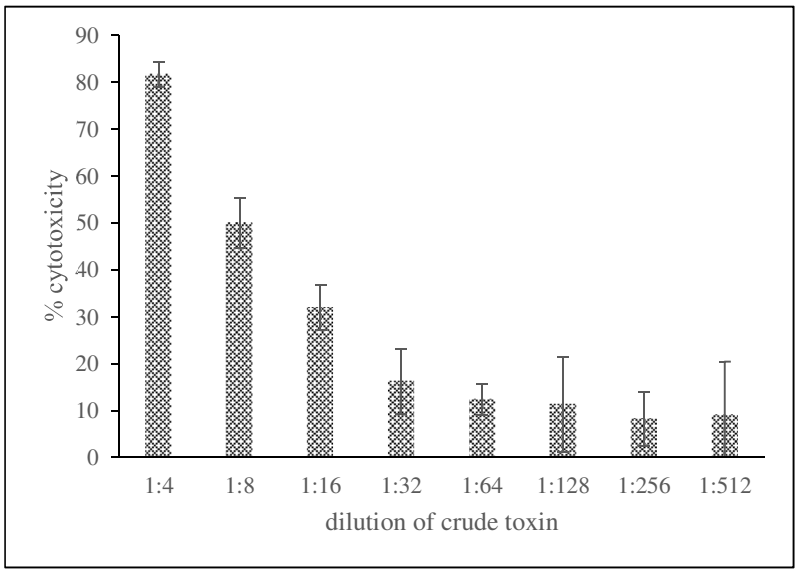

Fig 7. LMH cytotoxicity assay. Culture supernatant at several dilutions was prepared from field isolate cp58. Error bars depict standard deviation (SD). The amount of cytotoxicity induced by each dilution of crude toxin is expressed by average. The experiments were performed in triplicate.

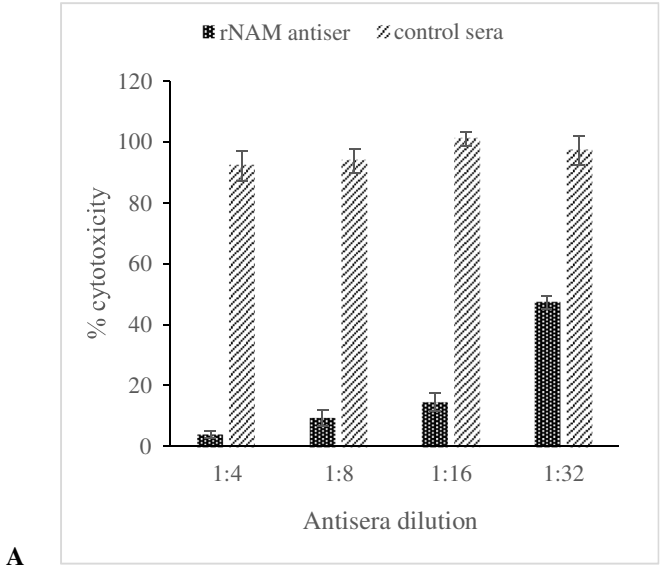

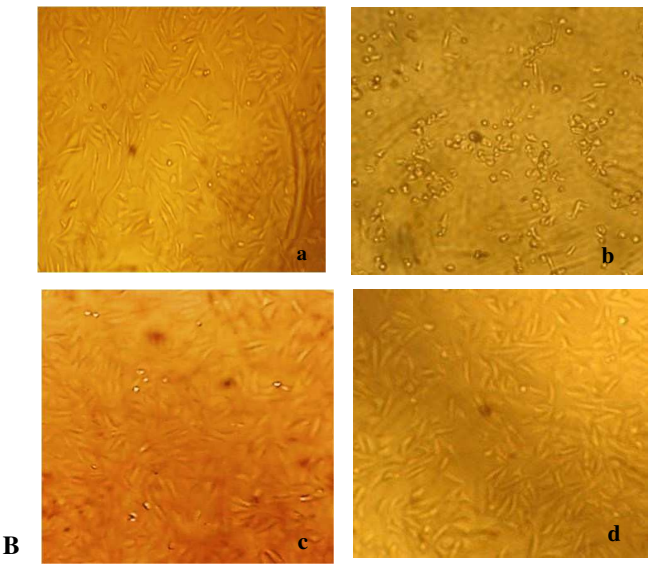

Fig 8. Neutralization of *C. perfringens* supernatant. Several dilutions of pre-immune sera and antisera raised against rNAM were incubated with Cp58 supernatant (2×LD 50) for 1 h at 37ºC. The mixture of toxin and sera were added to LMH cells and after 16 h incubation, cells viability was measured. (A) Cytopathic effects were expressed as percent of cytotoxicity. (B) Visually neutralization effects were illustrated, (a, c) negative control LMH cells before treatment, (b) crude toxin pretreated with pre-immune sera and (d) crude toxin pretreated with rabbit anti-NAM antisera. Cytopathic effects were visualized under a light microscope at 100 × magnification. The experiments were performed in triplicate and data are represented in mean ± S.D.

Supplementary data:

Table S1. Predicted continuous B-cell epitopes by ABCpred at threshold value above 0.5

Rank	position	Score	Rank	position	Score	Rank	position	Score
1	202-217	0.94	8	271-286	0.83	16	610-625	0.72
2	371-386	0.9	8	170-185	0.83	16	579-594	0.72
2	230-245	0.9	9	636-651	0.81	17	604-619	0.71
2	125-140	0.9	9	432-447	0.81	18	87-102	0.7
3	502-517	0.88	10	452-467	0.79	18	388-403	0.7
3	441-456	0.88	11	65-80	0.78	19	495-510	0.69
3	301-316	0.88	11	552-567	0.78	19	357-372	0.69
4	589-604	0.87	11	55-70	0.78	19	258-273	0.69
4	466-481	0.87	11	532-547	0.78	19	101-116	0.69
5	620-635	0.86	11	486-501	0.78	20	315-330	0.68
5	426-441	0.86	11	12-27	0.78	20	3-18	0.68
6	73-88	0.85	11	107-122	0.78	20	179-194	0.68

6	523-538	0.85	12	419-434	0.77	21	517-532	0.66
6	244-259	0.85	12	18-33	0.77	21	409-424	0.66
6	212-227	0.85	12	146-161	0.77	21	192-207	0.66
7	81-96	0.84	13	34-49	0.76	21	186-201	0.66
7	153-168	0.84	13	322-337	0.76	22	131-146	0.63
8	598-613	0.83	14	509-524	0.74	23	340-355	0.59
8	564-579	0.83	15	401-416	0.73	24	309-324	0.58
8	42-57	0.83	15	380-395	0.73			
8	287-302	0.83	15	332-347	0.73			

Table S2. Predicted continuous B-cell epitopes by BepiPred at threshold value above 0.5

position	Epitope sequence	position	Epitope sequence
13-55	NISVEGKTAGAGINASYNVQNTISY EQPDFRTIQRKDDANLAS	338-354	GFDNSKDVNSDFNFRIM
63-76	TKDGYNIDSYHAIY	380-385	QDAILA
85-107	RLYNNGDKNFTDDRDLSTLISGG	424-458	KTKTRITDQNIWENNTYPK VGLDDYSNNELYNKAD
156-157	TS	487-498	RERDFGNKNRED
168-178	WQDHKIEYYLA	524-529	IRVDDK
191-197	AAKEAAA	532	E
210-215	EKDAGT	535-566	AKYPKPDKKIYYLNDLAMN YKGDGFTDNAKVS
227-247	DGKTQEWEMDNPGNDFMTGSK	610-620	FVDTKSNLDED
255-262	KDENLKID	629-637	DRKLNTLNP
271-281	KRKYTAFPDAY	641-649	NALQPTLSV
305-328	SGNSTYNIKAEAAAKEAAAKEAAA		

Table S4. Predicted Discontinuous Epitopes using ElliPro server

Table S3. Predicted Discontinuous Epitopes using DiscoTope-2.0 server at threshold -1.

NO.	B-cell epitopes	score
1	$_{1}$MVSNSIGYSIGGNISVEGKTAGAGINASYNVQNTISYEQPDFK$_{43}$, $_{59}$KFVETKDGYNIDSYHAIYGNQLFMKSRLYNNGDKNFTDDRDLSTLISGGFS$_{109}$, $_{125}$DNDYILNIWETTQWRGTNKLSSTS$_{148}$	0.839
2	$_{504}$VVSDAMELDLTE$_{517}$, $_{526}$VDDKVKEDLAKYPKPDK$_{542}$, $_{554}$YKGDGFTDNAKVSVSTSGSGNIKLSFSVDDENKDNI$_{590}$, $_{596}$RRDGKV$_{602}$, $_{607}$NDSFVDYRKSNLDEDGVYVV$_{625}$, $_{629}$DRKENYLNFIEVNALQPTLSVNPVITLALGE$_{659}$	0.732
3	$_{275}$TAFPDAY$_{281}$	0.634
4	$_{444}$GLDDYSNNE$_{452}$, $_{520}$A, $_{523}$GIR$_{525}$	0.606
5	$_{48}$KDDAN$_{52}$	0.595
6	$_{338}$G, $_{339}$DNSKD$_{344}$, $_{347}$S, $_{404}$G, $_{485}$Q, $_{488}$ERDFGNKN$_{495}$, $_{497}$ED$_{498}$, $_{501}$K	0.584
7	$_{110}$PNMALALTAP$_{119}$, $_{121}$NAK$_{123}$, $_{168}$W	0.563
8	$_{144}$TL$_{145}$, $_{147}$R	0.556
9	$_{209}$GEKDA$_{213}$, $_{282}$KPENI$_{286}$	0.548
10	$_{194}$E, $_{224}$K, $_{259}$LKIDDI$_{264}$, $_{294}$YVVDKDI$_{300}$, $_{359}$N, $_{380}$QD$_{381}$, $_{384}$LA$_{385}$	0.542

Epitopes	Contact number	Epitopes	Contact number
$_{1}$MVSNSI$_{7}$	4,6,3,9,6,4,8	**$_{370}$N**	6
$_{29}$YNVQNTISYEQPDF$_{43}$	1,8,4,5,8,1,7,2,8,4,13,10,14,19,10	**$_{376}$R**	10
$_{45}$I	6	**$_{431}$D**	12
$_{59}$KFVETKDGYNIDSYHAIYGNQLFMKSRLYNNGDKNFTDDRDLSTLISG$_{107}$	11,27,15,12,22,11,17,3,22,8,13,2,2,4,3,20,0,8,17,23,19,13,24,25,28,14,11,6,9,7,10,2,10,0,8,24,12,20,3,6,5,15,17,23,4,19,24,10,2,6	**$_{433}$N**	4
$_{120}$K	0	**$_{446}$DD$_{447}$**	8,1
$_{134}$FDNDYILNIWETTQWRGTNKLSS$_{156}$	12,10,18,10,26,8,22,12,12,14,0,4,1,5,24,11,28,7,20,9,6,8,5,3	**$_{449}$SN$_{450}$**	3,7
$_{208}$SGEKDAGTDD$_{218}$	6,28,13,0,10,28,9,17,27,25,16	**$_{455}$NKADS$_{459}$**	11,5,0,14,8
$_{227}$D	7	**$_{490}$D**	2
$_{240}$N	1	**$_{492}$G**	1
$_{242}$F	1	**$_{494}$KN$_{495}$**	0,1
$_{258}$N	12	**$_{528}$DK$_{529}$**	0,2
$_{260}$K	9	**$_{555}$KGDG$_{558}$**	0,21,8,13
$_{270}$RKRKYTAFPDAYKPENIK$_{287}$	17,18,8,19,9,6,8,7,0,8,7,13,19,7,6,5,33,4	**$_{560}$TDN$_{562}$**	10,0,9
$_{341}$N	4	**$_{584}$DE$_{585}$**	0,9
$_{343}$KD$_{344}$	12,2	**$_{587}$KDN$_{589}$**	4,11,23
$_{347}$S	4	**$_{599}$G**	1
$_{349}$F	12	**$_{613}$T**	4
$_{359}$N	12		
$_{361}$SGG$_{363}$	6,1,17		

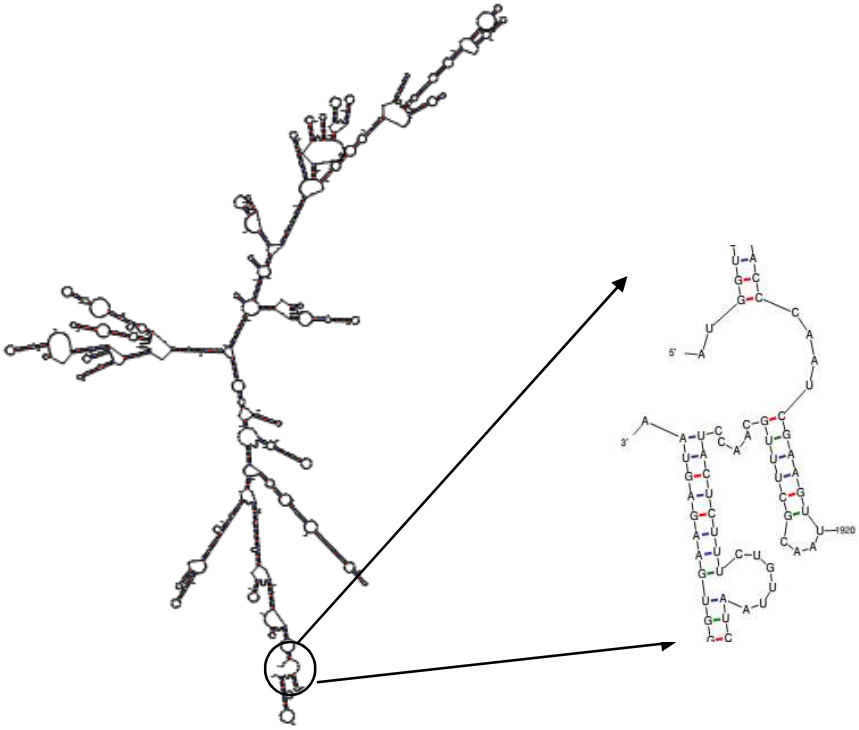

Fig. S5. Prediction of mRNA secondary structure using mfold server and start codon position.

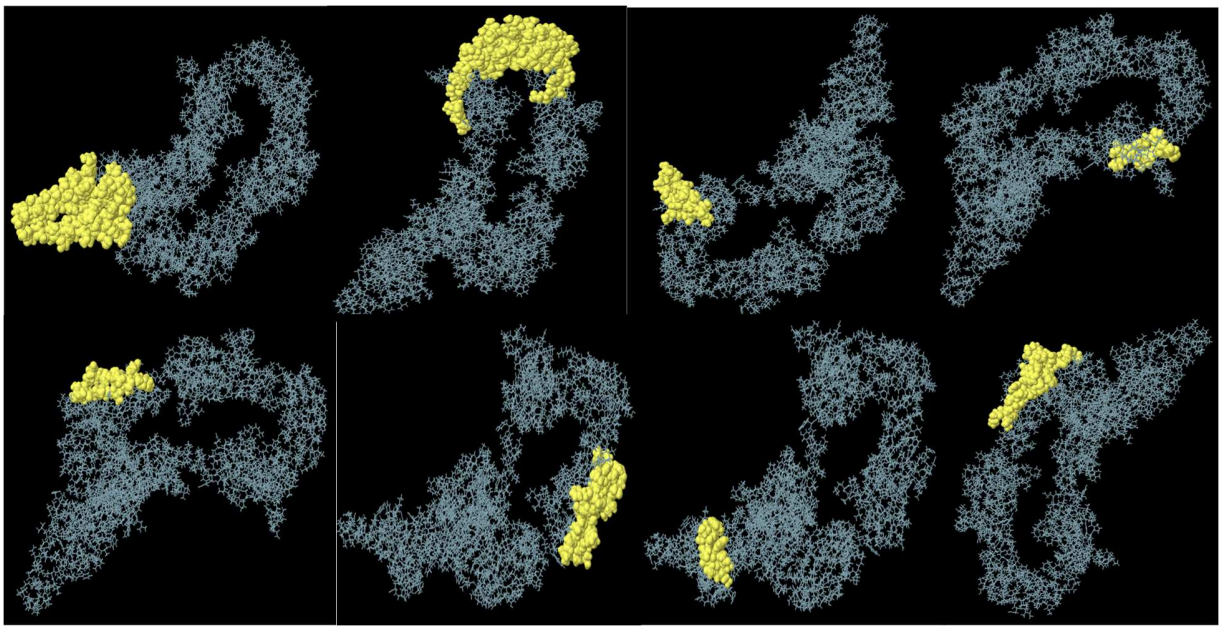

Fig. S6. Prediction of conformational B-cell epitopes by ElliPro that illustrated by Jmol.